

## ENERGY CALCULATION MODEL OF BALL KINEMATICS BASED ON BALL MILL COAL LOAD

YAN BAI<sup>1</sup>, FANG HE<sup>1</sup>, BINGYUN FU<sup>1</sup> AND XING HAN<sup>2</sup>

<sup>1</sup>School of Control and Computer Engineering  
North China Electric Power University  
No. 2, Beinong Rd., Huilongguan, Beijing 102206, P. R. China  
yunhangcanghai@163.com

<sup>2</sup>NARI Group Corporation Communication and Electricity Technology Branch  
Beijing 102200, P. R. China  
hf@ncepu.edu.cn

Received October 2013; revised February 2014

**ABSTRACT.** *There is not a more accurate and convenient solution pattern for the detection and control of coal load at present. The research on grinding medium used as a control parameter has not been reported. In order to improve the performance of coal load detection on balls' kinetic energy, a novel energy calculation model for ball kinematics based on coal load of ball mill is proposed in this paper. The operating conditions of ball mill and ball motion under the influence of coal load are analyzed carefully. The functional relations between the operating efficiency of coal pulverizing system, coal load and balls' kinetic energy are obtained. Origin and Matlab are utilized to establish the calculation model of real-time kinetic energy of balls with the increasing of coal load in cascading and projectile motion states. Meanwhile, a practical experiment is carried out to estimate the validity of the model. Results show that the kinetic energy model of balls is applicable for control of coal load in ball mills.*

**Keywords:** Coal load, Ball motion, Kinetic energy model, Control method

**1. Introduction.** The control of coal pulverizing system has drawn great attention but has not been well solved. Realizing automation of coal pulverizing system is of great significance in ensuring the safe and economical operation of equipment. The ball mill is an important part of coal pulverizing system and is widely applied in many industry fields. How to accurately detect and control coal load of ball mill is the key and technological difficulty [1,2]. It is obvious that the relevant published literature have focused on the studies of coal load detection as well as ball motion. During the study of coal load detection, several kinds of typical methods are presented, including differential pressure method, vibration method, noise method, ultrasonic inspection method and power method. In differential pressure method, coal load is expressed as import and export pressure difference of ball mill, and the measuring precision is finite under the influence of air rate. The fundamentals of vibration method are to analyze the relationship between vibration strength of system and coal load at a constant rotational speed of ball mill. However, the method has poor linearity and low accuracy. Noise method utilizes ball mill noise in detecting coal load, which has poor anti-interference ability and large deviation due to the effect of environmental noise except noise of mill cylinder on audio signals. Ultrasonic inspection method realizes coal detection by building relations between sending-receiving interval of ultrasonic and interface. The shortcomings of the method are existed in high system cost, demanding environmental requirements and lack of stability and reliability. Material levels are detected by the transformation rule of power and coal load in power

method. Nevertheless, the sensitivity of the method needs to be improved and it may be difficult to estimate coal load when power decreases [3-5]. Above mentioned methods cannot truthfully reflect coal load of ball mill because of significant limitations and low accuracy.

In the research of ball motion, a comprehensive coal grinding theory on the movement of projectile balls and equations of motion is given by E. W. Davis and H. B. Levinson [6,7]. R. Wang and R. E. McIvor estimate the effect of rotational speed of ball mill and material filling ratio on ball motion [8]. Other experimental studies including various factors like pure two-phase theory of motion may be presented in the literature [9-11]. It may be noted that most recent descriptions just discuss on the motion of material and impact of operating parameters.

In order to improve the performance of coal load control method, balls' kinetic energy is utilized to detect and control coal load in this paper, which avoids the influence of other factors and enhances the accuracy of coal detection. Meanwhile, this work establishes the kinetic energy model of balls with the increasing of coal load in cascading and projectile motion states. A practical experiment is carried out to estimate the validity of the model. In comparison to these existing coal load control methods, the energy model relates ball motion and coal load together, and analyzes ball kinematics under the influence of coal load. The approach provides the theoretical and experimental basis for a more convenient and effective control method of coal load based on balls' kinetic energy.

There are six parts in this paper. The first part is the summary of related work, the significance and motivation of the paper. The second and third parts present an analysis method for the preconditions, assumptions and operation parameters of ball mill to establish model. The fourth part is the energy calculation model which introduces ball motion under the influence of coal load and their functional relations. Experiments and result analysis are in the fifth part which shows the effectiveness of the novel model and coal load control method by comparing kinetic energy values. The major findings and innovation of the study are summarized finally in the conclusion.

**2. Operation Parameter Analysis of Ball Mill.** Ball motion in the coal mill is complicated but regular, which is determined by mill speed ratio, ball diameter and ball filling ratio. In order to further study the relationship between balls' kinetic energy and coal load, and establish kinetic energy model of balls based on coal load, operating parameters of ball mill are firstly analyzed and set. Figure 1 shows that balls reach the bottom of the mill in projectile motion state, so balls could effectively strike the fill area of medium.  $R$  is the distance between the ball regarded as a particle, and the center of ball mill. Since the ball radius is much smaller than the radius of ball mill, there is an approximate relation  $D = 2R$ , where  $D$  is the inner diameter of mill.  $\alpha$  is the included angle between  $OA$ , which is the line connecting the mill's center and the departure point, and the positive axis of the vertical axis  $Y$ .  $\beta$  is the included angle between  $OB$ , which is the line connecting the point of dropping and the center of the mill, and the positive axis of the horizontal axis  $X$ .

Critical speed  $n_c$  should be considered before other parameters are analyzed. In Figure 1, the following equation is satisfied in the departure point  $A$ .

$$mg \cos \alpha = mv^2/R \quad (1)$$

where,  $m$  is the ball quality,  $g$  is acceleration of gravity. Ignoring the sliding possibility, the ball's peripheral speed is equivalent to the coal mill's, that is  $v = n\pi R/30$ , where  $n$  is the working speed of the mill. Supposing that  $g = 9.81\text{m/s}^2$ , so  $\pi \approx \sqrt{g}$ , then there is

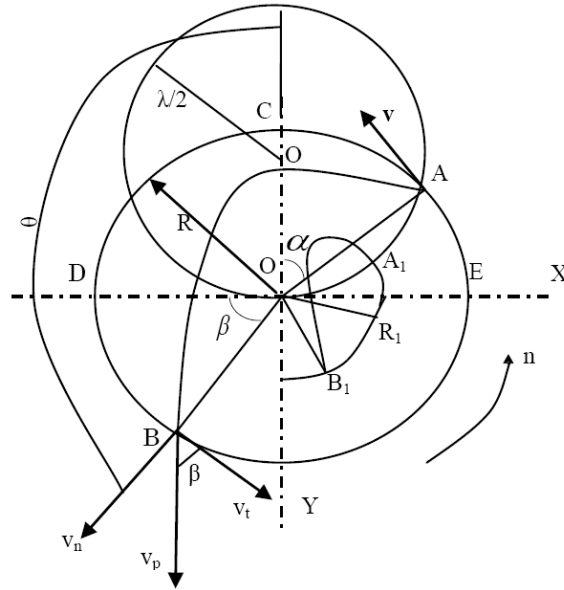


FIGURE 1. Track curve of projectile motion

the following equation [12].

$$\cos \alpha = (n/30)^2 R \tag{2}$$

When the ball is in centrifugal motion, and  $\alpha = 0$ , it reaches the highest point  $C$ . The ball reaches the critical speed  $n_c = 30/\sqrt{R} = 42.3/\sqrt{D}$ .

In practical, the mill speed ratio  $\Phi$  is the ratio of the mill's working speed  $n$  and the critical speed  $n_c$ . The ball filling ratio  $\Psi$  is the ratio of the ball's loose volume and the mill's effective volume. Both the mill speed ratio and the ball filling ratio determine the ball's motion and energy state. From Equation (2), we can conclude the following equation.

$$\Phi = \frac{n}{n_c} = \frac{30\sqrt{\cos \alpha}}{\sqrt{R}} \bigg/ \left( \frac{30}{\sqrt{R}} \right) = \sqrt{\cos \alpha} \tag{3}$$

Appropriate working speed should ensure that balls can reach the greatest dynamic energy when dropping. Supposing that the ball does the largest mechanical work when the departure angle  $\alpha = 54^\circ 45'$ ,  $\cos \alpha = 0.577$  and the optimal working speed  $n_{zj} = 22.8/\sqrt{R}$ . When  $n$  is close to  $n_{zj}$ ,  $\Phi$  is between  $[0.74, 0.8]$ .

In the coal mill's inputting energy, the consuming kinetic energy in the crash and friction between the ball and the mill, the ball and the coal contributes to the grinding capacity. Enlarging the mill's loading capacity can increase the percentage of the kinetic energy in balls' total energy. However, when the loading capacity is excessive, it also can limit the ball's motion and reduce the ball's kinetic energy. So there exists the optimum ball charge [13]. Also there exists an optimum ball filling ratio, and it is calculated by the following equation.

$$\Psi_{zj} = \frac{0.12}{\Phi^{1.75}} \tag{4}$$

The optimum ball charge is  $Q = \rho V \Psi_{zj} = \rho \pi D^2 L \Psi_{zj}$ .  $L$  is the mill's effective length.  $\rho$  is the balls' bulk density, and it normally indicates the percentage of ball's bulk volume in the total space volume. Balls occupy certain space volume, but there is certain gap among balls. Accumulation includes regular accumulation and random accumulation. The regular accumulation defines that the uttermost percentage of balls' bulk volume in the total space volume is 74%. The random accumulation defines that the uttermost

percentage of balls' bulk volume in the total space volume is 64%. Supposing the density of steel is  $7.8 \times 10^3 \text{ kg/m}^3$ , then  $\rho = 7.8 \times 10^3 \times 64\% = 4.9 \times 10^3 \text{ kg/m}^3$ , and the optimum ball charge [14,15] is determined by adjustment test. Supposing  $\Psi$  is between 10%-30%, and the ventilation volume and the coal fineness remain the same, the power consumption when the mill produces a ton coal is  $E_m = 0.3CQ$ .  $C$  is the proportionality coefficient, and  $Q$  corresponds to the smallest  $E_m$ .

Since the lifting height  $y = R \cos \alpha$ , the lifting height is different between large balls and small ones. The quality ratio between large balls and small ones is normally 3:1 or 4:1. The ball filling ratio [16] is calculated according to the following equation.

$$\Psi = \frac{4G}{\pi D^2 L \gamma} \tag{5}$$

where  $\gamma$  is balls' volume weight and calculated by  $\gamma = \sum 0.001 \times \text{balls' volume} \times \text{balls' ratio}$ . Therefore, ensuring the appropriate mill speed ratio, ball size and ball charge is significant to coal pulverizing efficiency.

**3. Analysis of Ball Motion and Coal Load.** The coal mill load is a significant factor influencing ball motion based on certain mill's rotational speed, ball diameter and ball charge. Figure 2 is the spatial distribution diagram describing that when the mill is rotating uniformly with dead axle, the coal mill load increases, where,

1)  $\Omega_1$  is the area of the circular and cascading motion. When the coal load in ball mill is little or almost empty, the ball and coal would do uniform circular motion with the mill or slide down. Besides, the chance of collision between balls is larger, and the motion between balls, coal and mill's liner plate is mainly grinding. Since the friction is enhanced, it leads to unnecessary balls and liner plate's abrasion, and the efficiency is low.

2)  $\Omega_2$  is the projectile motion area. When the coal load in ball mill is normal and not exceeding the falling point of balls' outermost layer, the motion between balls and coal in the underneath area is mainly striking. Therefore, it realized periodic circulatory crash between balls and coal, and it has high efficiency.

Suppose that: the volume of all the moving balls is  $\Omega = \Omega_1 + \Omega_2$ ,  $\rho$  is the balls' bulk density, and  $\Psi = \Omega / (\pi R^2 L)$  is the ball filling ratio. For the ball in the  $i$ th layer, its central angle is  $\sigma_i$ . According to the arc length computational formula, we can infer that  $d\Omega_1 = \pi R_i L \sigma_i / 180^\circ dR_i$ . The integration in the radius of the outermost layer  $R$  and the

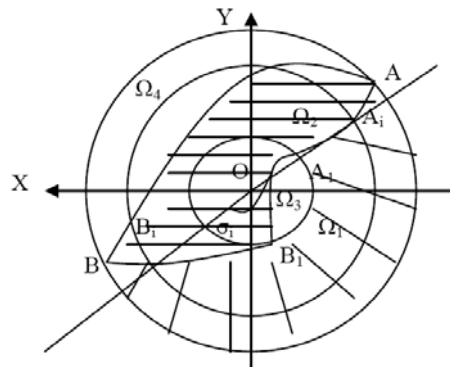


FIGURE 2. Distribution diagram of ball motion

innermost layer  $R_1$  is:

$$\Omega_1 = \frac{\pi L \sigma_i}{180^\circ} \int_{R_1}^R R_i dR_i = L \sigma_i \frac{\pi}{360^\circ} (R^2 - R_1^2) \quad (6)$$

And we can obtain that:

$$\Omega_2 = \Omega - \Omega_1 = \Psi \pi R^2 L - L \sigma_i \frac{\pi}{360^\circ} (R^2 - R_1^2) \quad (7)$$

where  $\sigma_i = 270^\circ - \alpha_i - \beta_i = 360^\circ - 4\alpha_i$ ,  $i = 1, 2, \dots$ .

3) In the area near the mill center region  $\Omega_3$ , the circling motion and the projectile motion mix up. The grinding and striking function is feeble since the ball motion is limited in  $\Omega_3$ .

4) Balls move in a circle or do not move in the blank region  $\Omega_4$ . When the mill is overloading, the balls' motion space is limited so that balls are not moving comparing with mill. Therefore, resources are wasted and the operation failure rate is increased in  $\Omega_4$  [17].

**4. Calculation Model for Balls' Kinetic Energy.** Balls have different motion curves with the increase of the coal load in the mill. Besides, balls' energy can be calculated in each state. There exists a relationship among balls' real-time kinetic energy, mill's coal load and operational efficiency. The ball charge in the mill consists of many layers of balls ( $i = 1, 2, \dots$ ). Now we take  $n$  ( $n \geq 1$ ) balls for example, whose radius is  $D_b$ . They are regarded as particles in mill's center of mass frame.

Assume that:

1) The crushed coal briquettes or particles are regarded as spheres when we consider the coal fineness.

2) The coal is fragile and brittle fractured under percussive action. Stress is in direct proportion to strain.

3) Coal briquettes or particles are in uniaxial stress state under stress or strike. The plane of fracture is parallel to the direction of pressure and cross the center of sphere.

4) Coal's mechanical properties are uniform.

5) Balls demonstrate their dynamic load properties when they crush coal. The capacity to resist dynamic load of coal is lower than resist static load. Let the ultimate strength for resisting pressure  $\sigma_s$  (static load) approximately convert the ultimate strength for resisting impact  $\sigma_d$  (dynamic load).

6) The interaction of balls in the same layer can be ignored since the falling velocity is equal inside the same layer.

**4.1. Kinetic energy model for the cascading motion.** When balls are rotating with the mill, they are comparatively static.  $G$  is the gravity of balls.  $N$  is the constraint reaction in the normal direction of cylinder wall.  $F$  is the force of friction. Therefore, the equation of motion is:

$$\begin{cases} mv^2/R = N - mg \cos(180^\circ - \alpha) \\ F = mg \sin(180^\circ - \alpha) \\ F \leq fN \end{cases} \quad (8)$$

where,  $f$  is the static friction coefficient between cylinder wall and balls. When  $\alpha$  is decreasing,  $N$  will decrease,  $F$  will increase and the component force in radial direction will gradually decrease. When  $\alpha = \alpha_1 = 90^\circ$ ,  $F$  reaches its maximum and balls begin sliding. When the coal load increases but does not exceed the quality of dash area  $\rho O_1$ , the motion of balls is regarded as deflection motion whose center of gravity is point  $S$ , and the angle is  $\theta$ , as shown in Figure 3. The quality of balls is  $M = \rho \Psi' \pi R^2 L$ , where

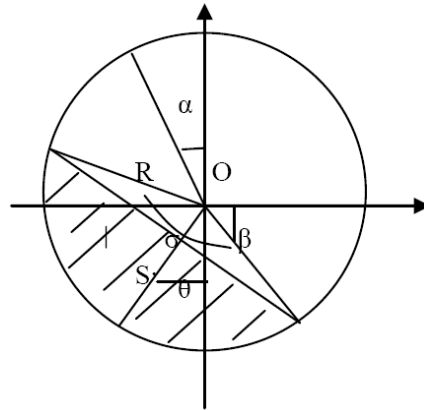


FIGURE 3. Analysis chart of circular and cascading motion

$\Psi'$  is the ball load ratio. The center of gravity  $S$  is on the angle bisector of the central angle  $\sigma$  which varies with coal load's uniformly increasing.  $OS$  is the distance between the center of gravity  $S$  and the center  $O$ . The following equation is based on the Pappus' theorem.

$$2\pi \cdot OS \cdot \Psi' \pi R^2 = \frac{4}{3} \pi \left( R \sin \frac{\sigma}{2} \right)^3 \tag{9}$$

We can calculate that:

$$OS = \frac{2R \sin^3 \frac{\sigma}{2}}{3\Psi'\pi} \tag{10}$$

So the kinetic energy of balls is calculated by the following equation:

$$E_k = \frac{1}{2} M v_S^2 = \frac{1}{2} \rho \Psi' \pi R^2 L (\omega \cdot OS)^2 = \frac{2\rho\pi LR^3 \cos \alpha \sin^6 \frac{\sigma}{2}}{9\Psi'} \tag{11}$$

With the increasing of coal load,  $S$  will gradually approach to the center  $O$  of the mill and  $OS$  will decrease. The kinetic energy of balls in area  $\Omega_1$  will gradually decrease from its initial value  $OS_0 = \frac{2R \sin^3 \frac{\sigma}{2}}{3\Psi'\pi}$ .

#### 4.2. The kinetic model for projectile motion.

4.2.1. *The kinetic calculation model for projectile motion.* When the coal load keeps increasing and exceeds  $\rho\Omega_1$ , balls begin to move relatively to the mill, and the equation of motion is as follows.

$$\begin{cases} mv^2/R = N - mg \cos(180^\circ - \alpha) \\ F - mg \sin(180^\circ - \alpha) = ma \\ F = f'N \end{cases} \tag{12}$$

where  $f'$  is the sliding friction coefficient between balls and the mill,  $a$  is the tangential acceleration of balls. When  $N = 0$ , Equation (1) is satisfied. When the ball rises to the point that  $\alpha = \alpha_2 = \arccos(n^2R/900)$ , it will separate from the cylinder wall and return to point  $B$  along the parabola [18]. The circular's center is  $O$  and radius is  $R$ , and its function is as follows.

$$x^2 + y^2 = R^2 \tag{13}$$

The ball's parabolic equation in  $xoy$  coordinate system can be converted as shown below based on the characteristics of the projectile motion.

$$y - y_A = \frac{v_{Ay}}{v_{Ax}}(x - x_A) - \frac{1}{2}g \left( \frac{x - x_A}{v_{Ax}} \right)^2 \tag{14}$$

i.e.,

$$y - R \cos \alpha = \frac{\sin \alpha}{\cos \alpha}(x + R \sin \alpha) - \frac{1}{2R \cos^3 \alpha}(x + R \sin \alpha)^2 \tag{15}$$

where,  $v_{Ax}$  and  $v_{Ay}$  are respectively the horizontal and vertical velocity components. Combining Equation (13) with (15), we can obtain the coordinate of the falling point  $B$  is  $(4R \sin \alpha \cos^2 \alpha - R \sin \alpha, -4R \sin^2 \alpha \cos \alpha + R \cos \alpha)$ .

Supposing that balls fall to  $B_i$ , where  $i$  is the projectile layer of balls,  $i = 1, 2, \dots$ , its velocity  $v_{pi}$  is divided into  $v_{ni}$  and  $v_{ti}$ .  $v_{ni}$  is the normal velocity component whose direction is from the mill center to the falling point  $B_i$ , and it strikes the coal.  $v_{ti}$  is the tangential velocity component which is tangential to mill's periphery, and it grinds the coal along the direction of cylinder wall's tangent line. Since balls rotate with the mill's center  $O$  and get in rolling motion, balls extrude and grind coal briquettes or grains in the contact zone between balls or the one between balls and the wall.

When the ball moves to the departure point  $A_i$ , its centrifugal force and normal force components are equal but in opposite directions. The ball will be in projectile motion by its own gravity. Striking is the main way to crush coal for balls while grinding is auxiliary, and the mill reaches its highest efficiency when balls strike the coal. Though the coordinates of  $A_i, B_i$  are different, they have the same geometric properties. According to Equation (2), we can obtain that  $R = \frac{900}{n^2} \cos \alpha = \lambda \cos \alpha$ , where  $\lambda$  is constant. Since each layer of balls has a departure point  $A_i$  and ball layer radius  $R_i$ , both of which conform to the equation above, the  $A_i$  set accords with the polar equation whose center is  $O_1$  and polar radius is  $OO_1 = \lambda/2$ . The polar equation is the track of departure points  $A_i$  set. Since  $\sin \beta_i = -\frac{y_{B_i}}{R} = 4 \sin^2 \alpha_i \cos \alpha_i - \cos \alpha_i$ , according to double angle formula  $\sin 2\alpha = 2 \sin \alpha \cos \alpha$  and  $\cos 2\alpha = \cos^2 \alpha - \sin^2 \alpha$ , we can obtain that  $\sin \beta_i = -\cos 3\alpha_i = \sin(3\alpha_i - 90^\circ)$ . Therefore, the polar angle is  $\theta_i = \beta_i + 90^\circ = 3\alpha_i$ , which is between the line  $OB_i$  and polar axis  $OY$ . The track of the falling point  $B_i$  is:

$$R_i = \lambda \cos \alpha_i = \lambda \cos \frac{\theta_i}{3} \tag{16}$$

Since  $R \sin \alpha_i < \lambda/2$  and  $R \cos \alpha_i < \lambda/2$ , the distance between ball's departure point  $A_i$  and the center of polar coordinate  $O_1$  is smaller than the polar radius [19]. In Figure 1,  $\lambda$  is a measured value which is the diameter of the circle which includes ball's departure point and represents the ball filling ratio. When  $\lambda$  gets smaller, then since the radius of the innermost layer gets smaller, the ball filling ratio gets larger. When the ball gets through the highest point  $C$  ( $R \sin \alpha_i \cos^2 \alpha_i - R \sin \alpha_i, 0.5R \sin^2 \alpha_i \cos \alpha_i + R \cos \alpha_i$ ) on its projectile track, we can obtain that  $v_{pyi} = \sqrt{2g(|y_{C_i}| + |y_{B_i}|)} = 3v_{ai} \sin \alpha_i$ . When the ball falls to point  $B$ , its kinetic energy is  $E_{ki} = \frac{1}{2}mv_{A_i}^2(9 - 8 \cos^2 \alpha_i)$ . Equation (17) is deduced by Equation (16).

$$\begin{aligned} E_{ni} &= \frac{1}{2}mv_{ni}^2 = \frac{1}{2}m \left( v_{xi} \cos \left( 3\alpha_i - \frac{\pi}{2} \right) + v_{yi} \sin \left( 3\alpha_i - \frac{\pi}{2} \right) \right)^2 \\ &= \frac{1}{2}64mv_{A_i}^2 \sin^6 \alpha_i \cos^2 \alpha_i \end{aligned} \tag{17}$$

According to the theory of E. W. Davis and H. B. Levinson, when the ball goes back to  $B_i$ , its normal velocity  $v_{ni}$  is calculated by the following equation. Besides, the ball's normal kinetic energy is  $E_{ni}$  in  $B_i$  and its quality is  $m$ .

$$E_{ni} = \frac{1}{2}mv_{ni}^2 = \frac{1}{2} \cdot \frac{\pi D_b^3 \rho}{6g} \cdot 64R_i g \sin^6 \alpha_i \cos^3 \alpha_i \tag{18}$$

The above equation only considers the ball in the  $i$ th layer at the position  $R_i$ . Balls in each layer are favorable but that does not mean that the total ball charge works favorably.

It is supposed that the quality of the balls concentrates on a certain layer called “middle polycondensation layer”. The “middle polycondensation layer” is the  $i_0$ th layer whose diameter is  $D_0$ . The following equation tells us the method of calculating point  $O$ 's polar rotational inertia for fan-shaped area.

$$R_0 = \sqrt{\frac{R^2 + R_1^2}{2}} = \sqrt{\frac{R^2 + (kR)^2}{2}} \quad (19)$$

where  $k = R_1/R$ , and it is related to the mill speed ratio  $\Phi$  and the ball filling ratio  $\Psi$ . When the ball in the “middle polycondensation layer” falls back to lining plate, its normal impact kinetic energy  $E_{ni_0}$  is calculated by the following equation since  $D_0 = 2R_0$ .

$$E_{ni_0} = \frac{16}{6}\pi D_b^3 \rho D_0 \sin^6 \alpha_{i_0} \cos^3 \alpha_{i_0} \quad (20)$$

Supposing  $s$  ( $s \geq 1$ ) is the amount of balls in the “middle polycondensation layer”, the total normal impact kinetic energy is calculated by the following equation.

$$E_n = s \frac{16}{6}\pi D_b^3 \rho D_0 \sin^6 \alpha_{i_0} \cos^3 \alpha_{i_0} \quad (21)$$

4.2.2. *Modified kinetic energy model for projectile motion.* In order to obtain Equation (21), we assumed certain conditions in initial calculation since these conditions are difficult to be quantified in equations. However, the influence of these conditions on balls' kinetic energy cannot be ignored. Equation (21) will produce large errors or even turn into worthless if we do not consider these conditions. Therefore, we introduce comprehensive empirical correction coefficient  $w$ , and it includes:

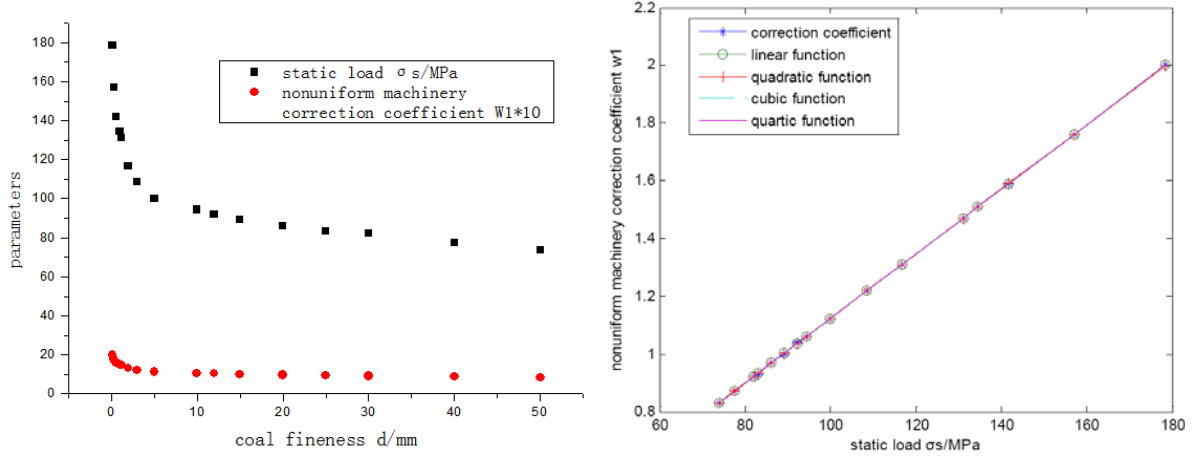
- 1) Coal's nonuniform mechanical properties are corrected, whose measured data are demonstrated in Table 1;
- 2) The process of grinding coal is effectively controlled and corrected, which includes the efficiency of coarse grinding and fine grinding;
- 3) Some factors such as the influence of the collision between balls and lining plate are corrected.

In Figure 4(a), since the nonuniform machinery correction coefficient  $w_1$  is numerically much smaller than coal particles' static load  $\sigma_s$ . In order to clearly observe the relationship between them,  $w_1$  is enlarged to 10 times and obtained by polynomial fitting. The polynomial fitting concludes that the high-order terms of quartic polynomial model coefficients are zero.  $[0, 1]$  is the measure index to comprehensively measure the regression model's fitting capacity for sample observations. The larger the coefficient of determination is, the better the independent variables' interpretation of the dependent variables is, and the higher the rate that variation caused by independent variables occupied in the total variation is [20-23]. Since the coefficient of determination can be reached up to 1 in this fitting model, the relationship between  $\sigma_s$  and  $w_1$  is not complicated under the

TABLE 1. Static load and nonuniform machinery correction coefficient based on coal fineness

coal fineness d/mm	50	40	30	25	20	15	12	10
$\sigma_s$ /MPa	73.85	77.43	82.11	83.13	86.19	89.15	92.13	94.35
$E_b$ /(N·mm)	722806.875	388017.216	173588.751	101704.360	53989.416	23559.002	12465.411	7387.605
$w_1$	0.83	0.87	0.92	0.93	0.97	1.00	1.04	1.06
coal fineness d/mm	5	3	2	1.2	1.0	0.6	0.3	0.15
$\sigma_s$ /MPa	99.86	108.53	116.79	131.07	134.64	141.78	157.08	178.50
$E_b$ /(N·mm)	977.380	229.444	73.158	17.735	10.543	2.398	0.333	0.048
$w_1$	1.12	1.22	1.31	1.47	1.51	1.59	1.76	2.00





(a) Scatter diagram for coal fineness, static load and nonuniform machinery correction coefficient (b) Relationship between static load and nonuniform machinery correction coefficient

FIGURE 4. Relevance of static load to nonuniform machinery correction coefficient based on coal fineness

condition of different coal fineness. We can observe the linear relationship in Figure 4(b). The equation is as follows:

$$w_1 = 0.0112\sigma_s + 0.0042 \tag{22}$$

Since it is hard to obtain the quantitative revised data for 2) and 3), we suppose that their degree of influence on balls' kinetic energy is equal to  $w_1$ , and then we can obtain the comprehensive empirical correction coefficient  $w = w_1^3$ . Equation (21) turns into the following Equation (23). The reasonableness of assumptions is tested by whether the balls' kinetic energy is not less than coal's anti-breaking energy  $E_b = \frac{1}{40}\pi\sigma_s d^3$  under the corresponding coal fineness.

$$E_n = ws \frac{16}{6} \pi D_b^3 \rho D_0 \sin^6 \alpha_{i_0} \cos \alpha_{i_0} \tag{23}$$

**5. Experimental Verification.** The practical ball motion is very complicated. The validity of the kinetic energy model in cascading and projectile motion with the increasing of the coal load is estimated by practical experiments. The experiments adopt the ball mill whose standard is  $0.325\text{m} \times 0.45\text{m}$ . The mill has rough rubber lining plate and its ball diameter is  $D_b = 0.1\text{m}$ , and the bulk density is  $\rho = 4.6\text{t/m}^3$ . The electronic speed controller controls the working speed of the mill, and the torque and speed sensor measures the mill's torque and the working speed [24]. It is assumed that the ball filling ratio in the experiment satisfies that the balls can move in cascading or projectile motion. The three-dimensional curve fitting in Matlab is researched to obtain the value of parameter  $k$  based on data in Table 2. In these experiments, the kinetic energy of ball motion reflects coal load in ball mill, whose random sampling of measured values and calculated values is demonstrated in the following Table 3.

From the comparison of calculated values and measured ones of ball mill, it can be seen that whether in cascading motion state of balls under the condition of little coal or projectile motion state of balls under the condition of the right amount of coal, calculated values are roughly identical to measured ones, and the model error is only 1%. Balls and coal characterized by loose are utilized as a whole in intimate contact with mill cylinder, whose centre of gravity is larger than the one in practice. The experimental as well as modeling techniques are presented to gain further insight to the law of calculated values slightly higher than measured ones. It is indicated that the more impact energy balls

TABLE 2. Values of  $k$  when the ball filling ratio is  $\Psi$  and the mill speed ratio is  $\Phi$ 

$\Psi/\%$ \backslash $\Phi/\%$	65	70	75	80	85	90	95	100
30	0.527	0.635	0.700	0.746	0.777	0.802	0.819	0.831
35	–	0.511	0.618	0.683	0.726	0.759	0.781	0.797
40	–	0.237	0.508	0.606	0.669	0.711	0.740	0.761
45	–	–	0.288	0.506	0.600	0.656	0.694	0.721
50	–	–	–	0.332	0.508	0.592	0.644	0.676

TABLE 3. Measured values and model values of single ball's kinetic energy based on different parameters

parameters/(t·m)	$\Psi/\%$	30		42	
	$\Phi/\%$	53.91	60.65	74.12	80.86
measured value		0.1429	0.1551	0.2092	0.2150
theoretical value		0.1566	0.1986	0.2143	0.2853

obtain in projectile motion state, the higher the grinding efficiency is. There exists close relevance between the operating efficiency of coal pulverizing system, coal load and real-time kinetic energy of balls. Furthermore, energy correction factor  $w$  can help derivation of formula be more close to material facts, so decreases the error between calculated and measured values.

**6. Conclusions.** The Balls' kinetic energy is utilized to detect and control coal load. Meanwhile, to study the relationship between the operating efficiency of coal pulverizing system, coal load and balls' kinetic energy, spacial distribution of balls in different motion states are presented. Several important conclusions may be drawn:

1) The operating conditions and process parameters are analyzed carefully in ball mill. With the increase of coal load, spacial distribution states of balls are described using multizone methods. Therefore, a close relationship between coal load of ball mill and ball movement is preliminary found. It is confirmed that projectile motion is the optimum state for balls to obtain the maximum kinetic energy, and there is the corresponding optimum coal load at the moment.

2) The energy calculation model in cascading and projectile motion states is established and the relative revision coefficient is given. Results of experiments show that the model only has the error of 1% for calculated values of balls' kinetic energy, so that the accuracy of which is verified. It is further indicated that balls' kinetic energy directly reflects the coal load. The approach provides the study with the theoretical basis for a novel optimum control method of coal load based on balls' kinetic energy.

3) Spacial distribution of balls is easy to be measured, so real-time kinetic energy of balls is obtained by the energy calculation model to adjust coal load of ball mill accordingly. It is shown that the kinetic energy model of balls is therefore applicable for controlling coal load in ball mills.

4) In comparison to these existing coal load control methods, a novel method based on balls' kinetic energy decreases the influence of other environmental factors on coal detection and enhances the accuracy of coal load control.

## REFERENCES

- [1] S. Rosenkranz, S. Breitung-Faes and A. Kwade, Experimental investigations and modeling of the ball motion in planetary ball mills, *Powder Technology*, vol.212, no.1, pp.224-230, 2011.
- [2] H. X. Jia, *Design and Operation of Coal Pulverizing System*, Water Resources and Electric Power Press, Beijing, 1995.
- [3] A. Zkan, M. Yekeler and M. Calkaya, Kinetics of fine wet grinding of zeolite in a steel ball mill in comparison to dry grinding, *Int. J. of Miner Process*, vol.90, no.1-4, pp.67-73, 2009.
- [4] S. Vladimir, P. Vsevolod and M. Galina, Energy efficient trajectories of industrial machine tools with parallel kinematics, *Proc. of the IEEE Int. Conf. on Industrial Technology*, Cape Town, South Africa, pp.1267-1272, 2013.
- [5] S. Masiuk and R. Rakoczy, Kinetic equation of grinding process in mixing of granular material using probability density functions, transient operators and informational entropy, *Chemical Engineering and Processing*, no.47, pp.200-208, 2008.
- [6] S. Y. Lu, Q. J. Mao, Z. Peng, X. D. Li and J. H. Yan, Simulation of ball motion and energy transfer in a planetary ball mill, *Chin. Phys. B*, vol.21, no.7, pp.1-9, 2012.
- [7] E. W. Davis, Fine crushing in ball mills, *AIME Trans.*, no.61, pp.250-296, 1919.
- [8] B. Ecevit and S. Brian, Population balance modeling of non-linear effects in milling processes, *Powder Technology*, vol.153, no.1, pp.59-71, 2005.
- [9] M. Boulvin, A. V. Wouwer, R. Lepore, C. Renotte and M. Remy, Modeling and control of cement grinding processes, *IEEE Trans. on Control Systems Technology*, vol.11, no.5, pp.715-725, 2003.
- [10] Y. S. Kwon, P. P. Choi, J. S. Kim and K. B. Gerasimov, Decomposition induced by mechanical milling, *Proc. of the 9th Russian-Korean International Symposium on Science and Technology*, Korus, pp.560-564, 2005.
- [11] H. Mori, H. Mio, J. Kano and F. Saito, Ball mill simulation in wet grinding using a tumbling mill and its correlation to grinding rate, *Powder Technology*, no.143-144, pp.230-239, 2004.
- [12] C. X. Zhang and W. P. Liu, Research on the law of the movement in the process of grinding, *Journal of Southern Institute of Metallurgy*, vol.21, no.2, pp.99-103, 2000.
- [13] J. F. Yue, J. Xiao and P. Qin, Experimental study of a dual inlet and outlet coal mill for reducing its milling power consumption, *Journal of Engineering for Thermal Energy and Power*, vol.26, no.3, pp.354-358, 2011.
- [14] X. B. Zhang, J. G. Yang and H. Zhao, Operation optimization of a ball mill pulverizing system, *Journal of Chinese Society of Power Engineering*, vol.30, no.2, pp.133-137, 2010.
- [15] Xi'an Electricity College, *Boiler Equipment and Operation*, Beijing Power Industry Press, Beijing, 1981.
- [16] W. D. Zheng, Calculation and determination of ball filling rate in ball mill, *East China Electric Power*, no.4, pp.42-44, 1996.
- [17] Q. H. Li, *Ore Crushing and Grinding*, Metallurgical Industry Press, Beijing, 1980.
- [18] G. J. Shi, *Study on Ball Mill's Medium Parameters Based on Three-dimensional Discrete Element Method*, Kunming University of Science and Technology, Kunming, China, 2008.
- [19] L. L. Ying, *Experimental Research of Kinematic Regularity of Mediums in Ball Mill*, Kunming University of Science and Technology, Kunming, China, 2009.
- [20] J. G. Wang, F. He and H. Di, Correlation analysis of magnetic field and conductivity, pH value in electromagnetic restraint of scale formation, *CIESC Journal*, vol.63, no.5, pp.1468-1473, 2012.
- [21] J. G. Wang, F. He, H. Di and Z. M. Xu, Influence of electromagnetic field on conductivity and pH value in fouling process, *Chemical Engineering (China)*, vol.41, no.1, pp.32-36, 2013.
- [22] Z. Y. Wang and L. Chen, Application of multiple linear regression statistical prediction model, *Statistics and Decision*, no.5, pp.46-47, 2008.
- [23] J. G. Wang, H. Di and F. He, Electromagnetic frequency influence on fouling resistance and electrical conductivity, *Control and Instruments in Chemical Industry*, vol.39, no.6, pp.761-764, 2012.
- [24] H. X. Tang, R. G. Zhang and R. Z. Zhang, Correction for theoretical calculation of useful power of ball mill, *Coal Mine Machinery*, no.2, pp.3-6, 1998.